Pathology - Research and Practice 215 (2019) 152388

Contents lists available at ScienceDirect

Pathology - Research and Practice

journal homepage: www.elsevier.com/locate/prp

Inhibitory effects of bortezomib in a subcutaneous tumor model of H22 mouse hepatocarcinoma cells

Mingao Zhu

Department of Oncology, the Second Affiliated Hospital of Soochow University, 1055 Sanxiang Road, Suzhou, Jiangsu, 215004, China

ARTICLE INFO

Keywords:
Liver cancer
Bortezomib
Subcutaneous xenograft
Efficacy
Apoptosis

ABSTRACT

Objective: To evaluate the inhibition effects and mechanism of bortezomib in a subcutaneous H22 mouse hepatocarcinoma model.

Methods: A subcutaneous xenograft model was constructed by subcutaneous injection of H22 cells in mice. The xenograft mice was randomly divided into bortezomib and control groups (n = 8 each). The bortezomib group was injected with 0.5 mg/kg bortezomib in saline via tail vein once every four days for a total of 4 times. The control group was intravenously given an equal volume of saline. The tumor size was measured every four days. At day 19, subcutaneous xenografts were obtained and the expression of apoptosis-related proteins in tumor was detected by immunochemical staining.

Results: The tumor volume of H22 xenografts in bortezomib group was significantly smaller than that in control group on day 19 ($p = 0.004$). The tumor volume/mouse weight ratio in bortezomib group was significantly lower compared with control group on day 13, 16 and 19 (all $p < 0.05$). The bortezomib group exhibited significantly higher expression of pro-apoptotic protein TNF-α ($p = 0.032$), and lower expression of anti-apoptotic protein XIAP, Stat3, and Survivin ($p = 0.024$, 0.016, and 0.039, respectively).

Conclusion: Bortezomib effectively inhibited the growth of H22 xenografts without affecting the mouse weight. The anti-tumor effects of bortezomib is associated with its stimulation on tumor cell apoptosis.

1. Introduction

Hepatocellular carcinoma (HCC) is a highly malignant tumor and is insensitive to most conventional chemotherapeutics [1]. Molecular targeted therapy is often the only treatment method in advanced HCC [2]. In recent years, molecular targeted therapy has attracted increasingly more attention for its good efficacy and safety in the treatment of advanced tumors. Tumor cell apoptosis involves a series of protein degradation processes, in which non-lysosome pathway is one of the main pathways in eukaryotic cells. Ubiquitin-proteasome pathway (UPP) is a process by which proteasome degrades the ubiquitin-modified proteins. Recent studies have found that UPP pathway is widely involved in cell cycle and cell apoptosis regulation. Abnormal activation of UPP is associated with tumor progression, drug resistance and immune escape [3,4]. Therefore, UPP pathway is often used as a molecular target for tumor treatment [5–7]. Bortezomib is the first reversible proteasome inhibitor approved by the FDA in 2003 for clinical use in the treatment of recurrent and refractory multiple myeloma [8]. It inhibits the activity of 26S proteasome and prevents I-kappa B serine phosphorylation and ubiquitination, thereby curbing the translocation of nuclear factor NF-kappa B into the nucleus for gene transcription, restraining cell proliferation and ultimately causing tumor cell apoptosis [9].

Clinical studies have shown that bortezomib could significantly inhibit the growth of adult T lymphocytic leukemia cells, and induce the apoptosis of chronic B lymphocytic leukemia cells, chronic myeloid leukemia cells as well as primary exudative lymphoma cells [10,11]. In recent years, there are several ongoing preclinical experiments using bortezomib in a variety of tumors, including non-small cell lung cancer, androgen-independent prostate cancer, kidney cancer, ovarian cancer, breast cancer, pancreatic cancer, and nasopharyngeal cancer [8,12]. However, researches on the efficacy and safety of bortezomib in liver cancer are rarely reported.

In our preliminary study, we found that bortezomib significantly inhibited the proliferation, migration and invasion of human liver cancer cells and induced apoptosis of these cells [13]. H22 is a mouse-derived liver cancer cell line that is widely used in liver cancer researches. In this study, we constructed H22 subcutaneous xenografts and evaluated the efficacy and safety of bortezomib in treating the liver cancer tumor.

E-mail address: mingaozhu53@hotmail.com.

https://doi.org/10.1016/j.prp.2019.03.017
Received 28 October 2018; Received in revised form 27 February 2019; Accepted 15 March 2019

2. Materials and methods

2.1. Cells and experimental animals

H22 hepatocarcinoma cells were obtained from the Department of Molecular Biology, Tongji Medical College, Huazhong University of Science and Technology. Six-week-old female KM mice weighting approximately 22 g were purchased from Hubei Experimental Animal Research Center (SCXK (E) 2008-0005). The animal experiments were approved by the Research Ethics Committee at the Huazhong University of Science and Technology and performed in strict accordance with the institutional and national regulations for the use of animals in research.

2.2. Determination of safe dosage

A total of 16 healthy KM mice were randomly divided into A and B groups (n = 8 each). In group A, each mouse was given 1 mg/kg bortezomib (LC Laboratories, Woburn, MA, USA) via tail vein injection every 4 days for twice. Mice in group B was given 0.5 mg/kg bortezomib every 4 days for twice. The mice were monitored for 14 days. Dead mice were subjected to anatomical examination.

2.3. Construction of subcutaneous xenograft model

A healthy KM mouse was intraperitoneally injected with 1×10^6 H22 cells. After a week, the mouse was sacrificed by cervical dislocation and soaked in 75% ethanol. Ascites fluid was collected, diluted with saline, and centrifuged at 1000 r/min for 5 min. The supernatant and red blood cells were removed. The H22 cells were rinsed 3 times with saline and prepared into cell suspension. To construct a subcutaneous xenograft model, 1×10^5 H22 cells were subcutaneously injected below the skin between the left hind limb and ventral abdomen. Palable tumor was clearly observed after 3 days and the tumor formation rate was 100%.

2.4. Grouping and treatment

A total of mice with subcutaneous xenografts were randomly divided into treatment and control group (n = 8). Starting from 3 days after injection, the treatment group was administered with 0.5 mg/kg bortezomib in saline via tail vein injection once every four days for a total of 4 times. The control group was intravenously given an equal volume of saline. The tumor size was measured every four days and tumor volume was calculated as length * width * width * 0.52 (cm^3), and each mouse was weighted.

2.5. Immunochemical analyses

At day 19 after tumor cell injection, mice were sacrificed by cervical dislocation and dissected. Subcutaneous xenografts were obtained, and subjected to formalin fixation, paraffin embedding, and sectioning. The expression of apoptosis-related proteins in tumor was detected by immunochemical staining. Briefly, the sections were deparaffinized in xylene, rehydrated with serial ethanol (100, 90, and 80% ethanol), and rinsed with running water. The sections were boiled in antigen retrieval solution for 5 min, and incubated in 3% hydrogen peroxide for 10 min to block the endogenous peroxidases. The sections were then blocked with 5% bovine serum albumin (BSA) for 20 min, and incubated with appropriate primary antibody overnight at 4℃. The sections were stained respectively with anti-XIAP (Santa Cruz Biotech., Dallas, TX, USA, 1:500 dilution), Survivin (Santa Cruz Biotech., 1:500 dilution), Stat3 (Cell Signaling Technology, Danvers, MA, USA, 1:500 dilution) and TNF-α (GeneTex, Irvine, CA, USA, 1:500 dilution). The sections were then rinsed and incubated with HRP-conjugated mouse anti-rabbit IgG antibody (Santa Cruz Biotech.) at 37℃ for 20 min followed by DAB color development for 5 min. The sections were further counterstained with hematoxylin and examined using a Zeiss axiovert 40 c inverted microscope. Yellow or brown-stained granules in cytoplasm and nuclei were identified as positive expression. The optical density (OD) of six randomly selected visual fields was quantified and the average optical density (IOD/area) was analyzed using the Image-Pro Plus 5.0 software. The experiment was repeated 3 times.

2.6. Western blot

Subcutaneous xenografts (150 mg) were collected for total protein extraction using RIPA lysis buffer (Beyotime, Shanghai, China). The protein concentration was determined using BCA protein assay kit (Beyotime). Protein samples were separated by 10% SDS-polyacrylamide gel electrophoresis (PAGE) and transferred to polyvinylidene difluoride membranes (Beyotime). After blocked with blocking buffer (Beyotime), membranes were incubated with appropriate dilutions of primary antibodies overnight at 4 °C: XIAP, Survivin, Stat3, TNF-α and β-actin (Santa Cruz Biotech.). The membranes were then incubated with horseradish peroxidase-conjugated secondary antibody at room temperature for 1 h. The bands were developed by chemiluminescence using the ECL detection system (GE Healthcare). The intensity of the bands was quantified using Image Lab software (Bio-Rad, Redmond, WA, USA). β-actin was used as the internal reference. The experiment was repeated 3 times.

2.7. Statistical analysis

Statistical analysis was performed using Prims5 statistical software. All data were expressed as mean ± SD of 3 independent experiments. Differences between the two groups were analyzed by student's t tests. p values smaller than 0.05 were considered statistically significant.

3. Results

3.1. Determination of safe dosage

According to previous studies, a 1 mg/kg bi-week intravenous dosage of bortezomib was recommended for mouse. We therefore tested the safety of bi-week 1 mg/kg and 0.5 mg/kg dosage. Results showed that 5 mice in 1 mg/kg group died by the end of safety experiment whereas no mice in 0.5 mg/kg died. The 5 dead mice were anatomically examined and abdominal hemorrhage was observed in these mice. Therefore, we decided to administrate mice a dose of 0.5 mg/kg once every four days for a total of 4 times in the current study.

3.2. Bortezomib inhibits the tumor growth

A subcutaneous xenograft model was established by subcutaneous injection of 1×10^5 H22 cells into 16 healthy mice (day 1). After 3 days, the tumor formation was observed in all 16 mice, resulting in a tumor formation rate of 100%. The tumor volume was monitored on day 4, 7, 10, 13, 16 and 19. It was found that the tumor volume in control group was increased exponentially. In contrast, the tumor growth in bortezomib group was effectively inhibited. By day 19, the tumor volume in bortezomib group was significantly smaller compared with control group ($p = 0.004$, Fig. 1).

3.3. Bortezomib did not affect the weight of mice

On day 19, mice were sacrificed and tumor samples were obtained. In bortezomib group, one mouse died on day 12 due to unkown reason, the tumor in 1 mouse disappeared, and the tumor in 1 mouse was not isolated due to extensive infiltration. In control group, the tumor in 3 mice was not isolated due to extensive infiltration. As a result, 5 xenografts were isolated from each group (Fig. 2). The tumor volume/

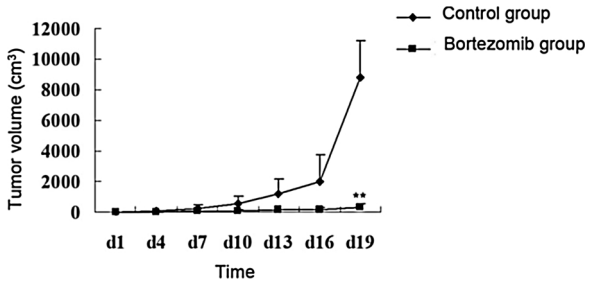

Fig. 1. Comparison of tumor growth between the two groups. On day 4, 7, 10, 13, 16 and 19 days after subcutaneous injection of H22 cells in mice, the tumor volume was measured as length * width * width * 0.52 (cm^3). **, $p < 0.01$ compared with control group.

mouse weight ratios in control group were 2.29 ± 0.94, 8.16 ± 5.28, 16.92 ± 12.38, 32.592 ± 28.93, 55.01 ± 51.05, respectively, and 2.31 ± 1.29, 1.09 ± 0.37, 0.53 ± 0.14, 0.40 ± 0.20, 0.34 ± 0.19, respectively in bortezomib group. As shown in Fig. 2C, the average tumor volume/mouse weight ratio in bortezomib group was significantly lower than that in control group on day 13, 16 and 19 (all $p < 0.05$).

3.4. Bortezomib stimulated pro-apoptotic protein expression and inhibited anti-apoptotic protein expression

Immunochemical analyses of subcutaneous xenografts showed that the bortezomib group exhibited significantly higher expression of pro-apoptotic protein TNF-α ($p = 0.032$), and lower expression of anti-apoptotic protein XIAP, Stat3, and Survivin ($p = 0.024$, 0.016, and 0.039, respectively) when compared with control group (Fig. 3 and Table 1). Consistently, Western blot analyses of TNF-α, XIAP, Stat3, and Survivin expression in bortezomib group also showed similar pattern of change when compared with control group (Fig. 4), suggesting that bortezomib might inhibit tumor growth via stimulating pro-apoptotic protein expression and inhibiting anti-apoptotic protein expression.

4. Discussion

Molecular targeted therapy has recently become the biggest focus in the field of liver cancer treatment [14]. Bortezomib is a dipeptidyl boric acid compound that binds directly to proteasome 20S subunit and blocks the activity of the enzyme, thus rapidly and reversibly impeding the proteasome pathway [15,16]. Pre-clinical studies have shown that malignant tumor cells are more sensitive to bortezomib than normal cells [17–20], which makes it a highly potent molecular targeted drug. In our preliminary study, we found that bortezomib significantly inhibited the proliferation, migration and invasion of human liver cancer cells and induced apoptosis of these cells [13]. We therefore investigated the inhibitory effects of bortezomib in a subcutaneous tumor model of H22 mouse hepatocarcinoma cells in this study, and found that bortezomib effectively inhibited the growth of xenografts without affecting the mouse weight. All together, these results suggested that bortezomib inhibited the liver tumor growth. The conventional administration of 1 mg/kg bortezomib biweekly via tail vein injection was found toxic as described in the literature. High-dose drug may cause anorexia and emaciation, or even anemia, hemorrhage and death in severe conditions, leading to high mortality rate. Safety test suggested bi-week 0.5 mg/kg bortezomib did not cause death of mice. Therefore, the dose of bortezomib in this study was reduced to 0.5 mg/kg.

Due to various environmental and genetic factors, normal cells loss the apoptosis ability, which has been considered as one of the key factors in the occurrence and development of cancer [21]. Stimulating and restoring the apoptosis ability of tumor cells has become an effective way to cure cancer [22]. The immunohistochemical results in our study showed that bortezomib had stimulating pro-apoptotic protein expression (TNF-α) and inhibiting anti-apoptotic protein expression (XIAP, Stat3, and Survivin), suggesting that bortezomib might promote the apoptosis of tumor cells through regulating the expression of apoptosis-related proteins, and thus inhibit the growth of subcutaneous H22 xenografts. This action mechanisim is consistent with the that of proteasome inhibitors. STAT3 is one of the most investigated apoptosis-related proteins [23,24]. Over-expression of STAT3 has been reported in tumor cells [25,26]. STAT3 phosphorylation (activation state) in human HCC samples is close to 60%, suggesting that STAT3 activation may be associated with the malignant degree and prognosis of HCC [27]. Nevertheless, the role and molecular mechanism of bortezomib in liver cancer needs further in-depth investigation.

In summary, we constructed an H22 subcutaneous xenografts in a mouse model and found that bortezomib effectively inhibited the growth of xenografts without affecting the mouse weight. We also found that bortezomib had significantly stimulated the expression of

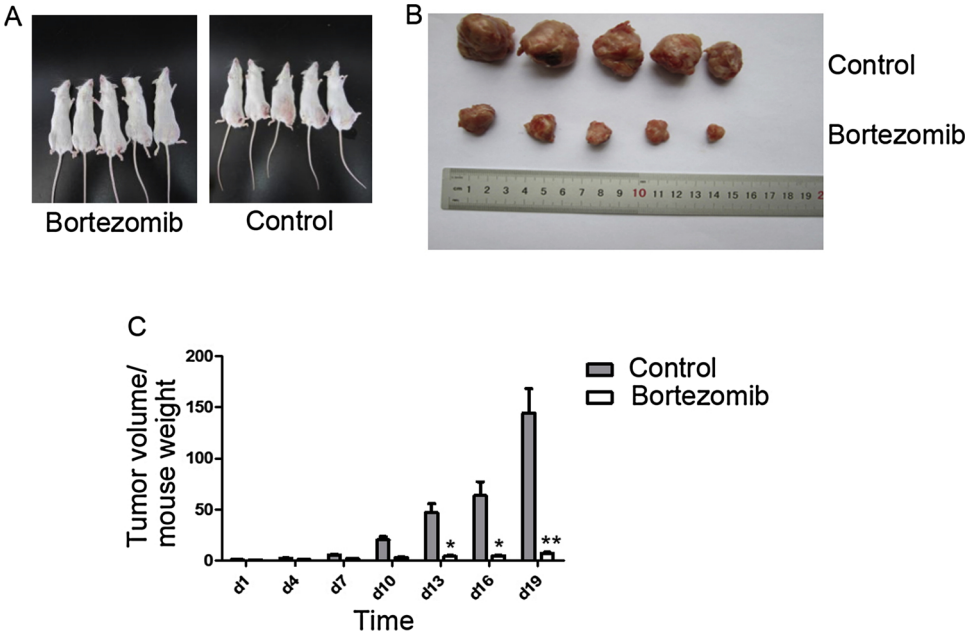

Fig. 2. Comparison of subcutaneous xenografts between the group. On day 19 after subcutaneous injection of H22 cells, 5 mice (A) from each group were sacrificed. The bortezomib group had significantly smaller size of xenografts (B) and lower tumor volume/mouse weight ratio (C) compared with control group. *, $p < 0.05$ and **, $p < 0.01$ compared with control group.

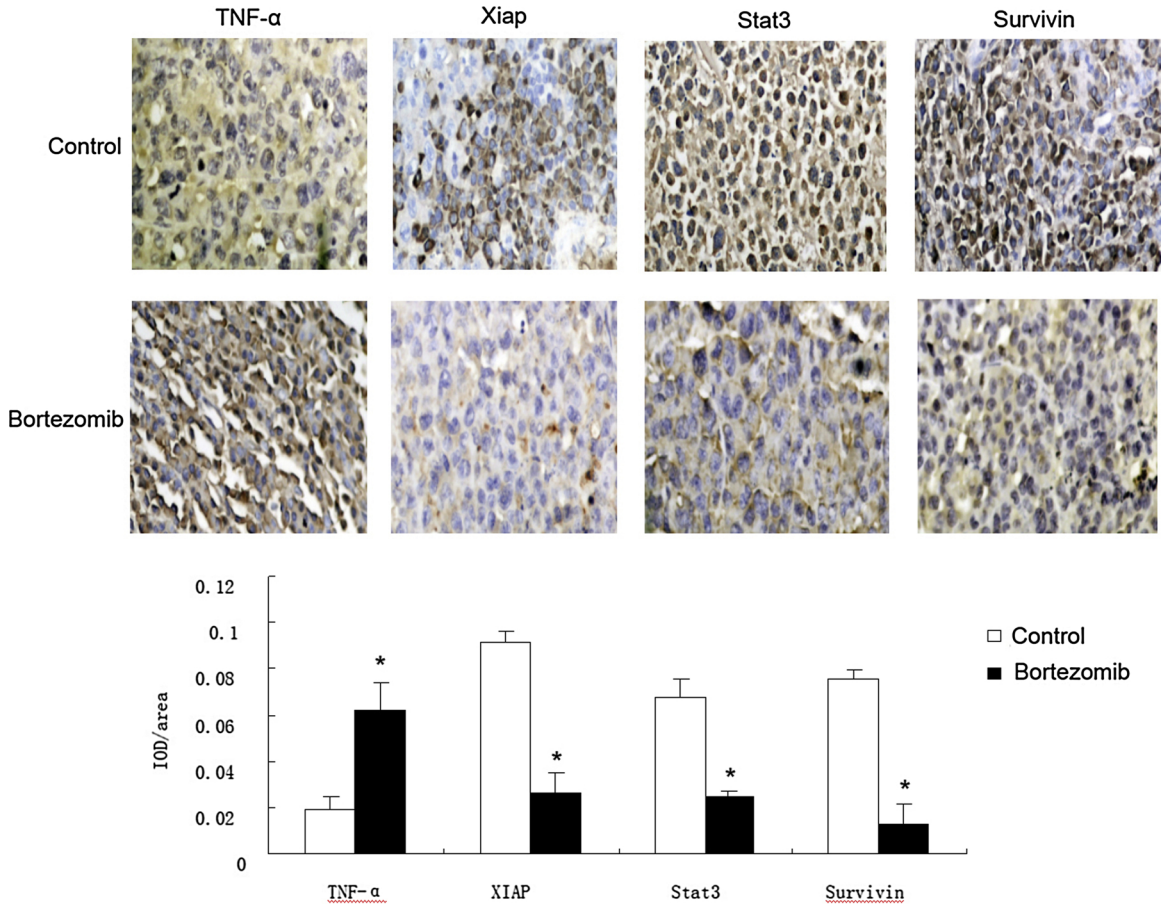

Fig. 3. Immunochemical analyses of apoptosis-related protein expression in subcutaneous xenografts. On day 19 since subcutaneous injection of H22 cells, subcutaneous xenografts were isolated and subjected to immunochemical staining. The bortezomib group had significantly increased expression of pro-apoptotic protein TNF-α, and decreased expression of anti-apoptotic protein XIAP, Stat3, and Survivin. *, $p < 0.05$ compared with control group.

Table 1
Immunichemical analyses of the expression of apoptosis-related proteins TNF-α, Xiap, Stat3 and Survivin.

Group	n	TNF-α(IOD/Area)	Xiap(IOD/Area)	Stat3(IOD/Area)	Survivin(IOD/Area)
Control	8	0.019 ± 0.006	0.091 ± 0.009	0.067 ± 0.002	0.076 ± 0.009
Bortezomib	8	0.062 ± 0.012	0.026 ± 0.005	0.025 ± 0.008	0.012 ± 0.003

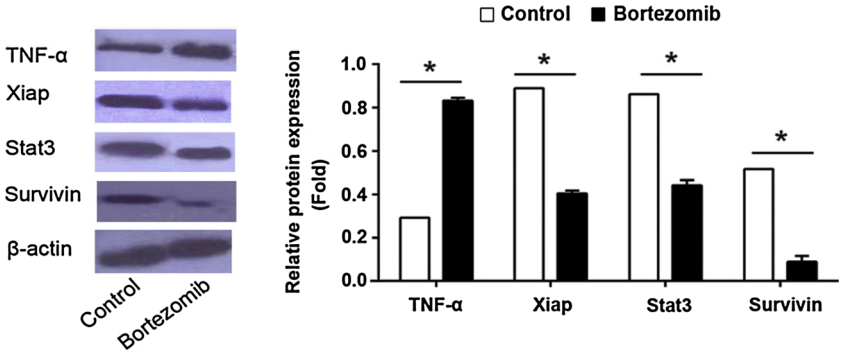

Fig. 4. Western blot analyses of apoptosis-related protein expression in subcutaneous xenografts. On day 19 since subcutaneous injection of H22 cells, total protein was extracted from subcutaneous xenografts and analyzed by Western blot. The bortezomib group had significantly increased expression of pro-apoptotic protein TNF-α, and decreased expression of anti-apoptotic protein XIAP, Stat3, and Survivin. *, $p < 0.05$ compared with control group.

pro-apoptotic protein TNF-α, and inhibited the expression of anti-apoptotic protein XIAP, Stat3, and Survivin, suggesting the anti-tumor effects of the drug is associated with its stimulation on tumor cell apoptosis. The current study has provided a theoretical basis for using bortezomib in liver cancer treatment. However, clinical trials will be needed to warrant the clinical application of the drug.

Data availability

Data will be available upon request.

Conflict of interests

None.

References

[1] R.L. Siegel, K.D. Miller, A. Jemal, Cancer statistics, 2017, CA Cancer J. Clin. 67 (2017) 7–30.
[2] H.B. El-Serag, Hepatocellular carcinoma, N. Engl. J. Med. 365 (2011) 1118–1127.
[3] D. Chen, Q.P. Dou, The ubiquitin-proteasome system as a prospective molecular target for cancer treatment and prevention, Curr. Protein Pept. Sci. 11 (2010) 459–470.
[4] J. Adams, Preclinical and clinical evaluation of proteasome inhibitor PS-341 for the treatment of cancer, Curr. Opin. Chem. Biol. 6 (2002) 493–500.
[5] J. Yan, H. Li, S. Li, et al., The Arabidopsis F-box protein CORONATINE INSENSITIVE1 is stabilized by SCFCOI1 and degraded via the 26S proteasome pathway, Plant Cell Online 25 (2) (2013) 486–498.
[6] L. Dalla Via, C. Nardon, D. Fregona, Targeting the ubiquitin-proteasome pathway with inorganic compounds to fight cancer: a challenge for the future, Future Med. Chem. 4 (4) (2012) 525–543.
[7] J. Yin, J.M. Zhu, X.Z. Shen, The role and therapeutic implications of RING-finger E3 ubiquitin ligases in hepatocellular carcinoma, Int. J. Cancer 136 (2) (2015) 249–257.
[8] D. Chen, M. Frezza, S. Schmitt, et al., Bortezomib as the first proteasome inhibitor anticancer drug: current status and future perspectives, Curr. Cancer Drug Targets 11 (March 3) (2011) 239–253.
[9] F. Accardi, D. Toscani, M. Bolzoni, et al., Mechanism of action of Bortezomib and the new proteasome inhibitors on myeloma cells and the bone microenvironment: impact on myeloma-induced alterations of bone remodeling, Biomed Res. Int. 2015 (2015) 1–13.
[10] B. Holkova, V. Yazbeck, M. Kmieciak, et al., A phase 1 study of bortezomib and romidepsin in patients with chronic lymphocytic leukemia/small lymphocytic lymphoma, indolent B-cell lymphoma, peripheral T-cell lymphoma, or cutaneous T-cell lymphoma, Leuk. Lymphoma 58 (6) (2017) 1349–1357.
[11] A.R. Walker, H. Wang, K. Walsh, et al., Midostaurin, bortezomib and MEC in relapsed/refractory acute myeloid leukemia, Leuk. Lymphoma 57 (9) (2016) 2100–2108.
[12] Z. Huang, Y. Wu, X. Zhou, et al., Efficacy of therapy with bortezomib in solid tumors: a review based on 32 clinical trials, Future Oncol. 10 (10) (2014) 1795–1807.
[13] M. Zhu, Inhibitory Effects and Mechanism of Bortezomib on Liver Cancer Cells, Dissertation of Soochow University, 2014.
[14] K.W. Chen, T.M. Ou, C.W. Hsu, et al., Current systemic treatment of hepatocellular carcinoma: a review of the literature, World J. Hepatol. 7 (June 10) (2015) 1412–1420.
[15] R. Farra, B. Dapas, D. Baiz, F. Tonon, S. Chiaretti, G. Del Sal, et al., Impairment of the Pin1/E2F1 axis in the anti-proliferative effect of bortezomib in hepatocellular carcinoma cells, Biochimie 112 (2015) 85–95.
[16] F. Accardi, D. Toscani, M. Bolzoni, et al., Mechanism of action of Bortezomib and the new proteasome inhibitors on myeloma cells and the bone microenvironment: impact on myeloma-induced alterations of bone remodeling, Biomed Res. Int. 2015 (2015) 1–13.
[17] A. Pal, M.A. Young, N.J. Donato, Emerging potential of therapeutic targeting of ubiquitin-specific proteases in the treatment of cancer, Cancer Res. 74 (2014) 4955–4966.
[18] I. Saeki, S. Terai, K. Fujisawa, T. Takami, N. Yamamoto, T. Matsumoto, et al., Bortezomib induces tumor-specific cell death and growth inhibition in hepatocellular carcinoma and improves liver fibrosis, J. Gastroenterol. 48 (2013) 738–750.
[19] Huang I-Tao, Bijay Dhungel, Ritu Shrestha, et al., Spotlight on bortezomib: potential in the treatment of hepatocellular carcinoma, Expert Opin. Investig. Drugs (2018).
[20] K.K. Ciombor, Y. Feng, A.B. Benson 3rd, Y. Su, L. Horton, S.P. Short, et al., Phase II trial of bortezomib plus doxorubicin in hepatocellular carcinoma (E6202): a trial of the Eastern Cooperative Oncology Group, Invest. New Drugs 32 (2014) 1017–1027.
[21] S.W. Lowe, A.W. Lin, Apoptosis in cancer, Carcinogenesis 21 (2000) 485–495.
[22] J.M. Schattenberg, M. Schuchmann, P.R. Galle, Cell death and hepatocarcinogenesis: dysregulation of apoptosis signaling pathways, J. Gastroenterol. Hepatol. 26 (Suppl 1) (2011) 213–219.
[23] JieYuan, Fei Zhang, Ruifang Niu, Multiple regulation pathways and pivotal biological functions of STAT3 in cancer, Sci. Rep. 5 (2015) 17663.
[24] N. Fathi, G. Rashidi, A. Khodadadi, et al., STAT3 and apoptosis challenges in cancer, Int. J. Biol. Macromol. 117 (2018) 993–1001.
[25] Y. Pan, S. Wang, B. Su, et al., Stat3 contributes to cancer progression by regulating Jab1/Csn5 expression, Oncogene 36 (8) (2017) 1069–1079.
[26] M. Tong, J. Wang, N. Jiang, et al., Correlation between p-STAT3 overexpression and prognosis in lung cancer: a systematic review and meta-analysis, PLoS One 12 (8) (2017) e0182282.
[27] C. Zhang, F. Guo, G. Xu, J. Ma, F. Shao, STAT3 cooperates with Twist to mediate epithelial-mesenchymal transition in human hepatocellular carcinoma cells, Oncol. Rep. 33 (2015) 1872–1882.